

Physics with tagged forward protons at the LHC

V.A. Khoze^{1,2}, A.D. Martin¹, M.G. Ryskin^{1,2}

¹ Department of Physics and Institute for Particle Physics Phenomenology, University of Durham, Durham, DH1 3LE, UK

² Petersburg Nuclear Physics Institute, Gatchina, St. Petersburg, 188300, Russia

Received: 15 March 2002 /

Published online: 21 June 2002 – © Springer-Verlag / Società Italiana di Fisica 2002

Abstract. We emphasize the importance of tagging the outgoing forward protons to sharpen the predictions for New Physics at the LHC (such as the diffractive production of a light Higgs boson). The rescattering effects lead to a rich distinctive structure of the cross section as a function of the transverse momenta of the protons. We show that a study of the correlations between the proton transverse momenta for double-diffractive production of central dijets will provide a detailed check of the whole diffractive formalism. Adopting a perturbative two-gluon structure of the Pomeron, we emphasize that 2^{++} quarkonium production, via Pomeron-Pomeron fusion, is strongly suppressed. This offers a favourable production mechanism for non- $q\bar{q}$ states, such as glueballs.

1 Introduction

Exclusive double-diffractive-like processes of the type

$$pp \rightarrow p + M + p \quad (1)$$

can significantly increase the physics potential of high energy proton colliders. Here M represents a system of invariant mass M , and the $+$ signs denote the presence of rapidity gaps which separate the system M from the protons. Such processes allow, on the one hand, novel studies of QCD and of the diffractive amplitude at very high energies, while, on the other hand, allow an exceptionally clean experimental environment to identify New Physics signals (such as the Higgs boson, SUSY particles, etc., see [1] and therein). Moreover tagging two forward protons offers an attractive extension of the proton collider physics programme to studies of high-energy $\gamma\gamma$ collision physics; see, for example, [1–3].

In such events we produce a colour-singlet state M which is practically free from soft secondary particles. Moreover, if forward going protons are tagged we can reconstruct the ‘missing’ mass M with good resolution, and so have an ideal means to search for new resonances and to study threshold behaviour phenomena. We have to pay a price for ensuring such a clean diffractive signal. In particular, the diffractive event rate is suppressed by the small probability, \hat{S}^2 , that the rapidity gaps survive soft rescattering effects between the interacting hadrons, which can generate secondary particles which populate the gaps [4–12].

In general, we may write the survival factor \hat{S}^2 in a multi-channel eikonal framework in the form

$$\hat{S}^2 = \frac{\int \sum_i |\mathcal{M}_i(s, b_t^2)|^2 \exp(-\Omega_i(s, b_t^2)) d^2 b_t}{\int \sum_i |\mathcal{M}_i(s, b_t^2)|^2 d^2 b_t} \quad (2)$$

where the incoming proton is decomposed into diffractive eigenstates, each with its own opacity¹ Ω_i . The amplitudes $\mathcal{M}_i(s, b_t^2)$ of the process of interest may be different in the different diffractive eigenstates. They are expressed in impact parameter b_t space at centre-of-mass energy \sqrt{s} . It is important to recall that the suppression factor \hat{S}^2 is not universal, but depends on the particular hard subprocess, as well as on the kinematical configurations of the parent reaction, see, for example, [12].

Double-diffractive Higgs production,

$$pp \rightarrow p + H + p, \quad (3)$$

at the LHC, is a good example of illustrating the pros and cons of such exclusive processes. Let us assume a Higgs boson of mass $M_H = 120$ GeV and consider detection in the $b\bar{b}$ decay channel. The disadvantage is that to ensure the survival of the rapidity gaps in (3), the predicted cross section is low, $\sigma \simeq 2$ fb, corresponding to a survival factor $\hat{S}^2 = 0.02$. The advantage is that, *by tagging the outgoing protons*, the signal-to-background ratio² is extremely favourable relative to other Higgs signals [9, 13],

$$\frac{\text{signal } (H \rightarrow b\bar{b})}{b\bar{b} \text{ QCD background}} \gtrsim 4, \quad (4)$$

¹ Really we deal with a matrix $\Omega_{jj'}^{ii'}$, where the indices refer to the eigenstates of the two incoming and two outgoing hadrons [12]

² The ratio quoted in (4) corresponds to a cut on the b jet transverse momenta of $p_t(b) > 0.4M_H$

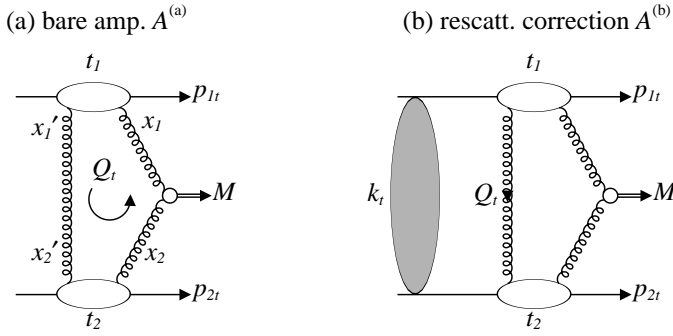


Fig. 1a,b. The bare amplitude $A^{(a)}$ and the rescattering correction $A^{(b)}$ for the double-diffractive process $pp \rightarrow p + M + p$

if the missing mass resolution ΔM obtained by the proton taggers is 1 GeV. Indeed, with dedicated forward proton spectrometers at the LHC, the process $pp \rightarrow p + H + p$ may even be the light Higgs discovery channel.

For completeness, we note that for Higgs production via photon-photon fusion, the survival factor is much larger, $\hat{S}^2 \simeq 0.86$ [1,3], and the corresponding cross section $\sigma_{\gamma\gamma}(H \rightarrow b\bar{b}) \simeq 0.1$ fb. In this case the signal-to-background ratio is

$$\frac{\text{signal } (\gamma\gamma \rightarrow H \rightarrow b\bar{b})}{b\bar{b} \text{ QED background}} \simeq \frac{7 \text{ GeV}}{\Delta M_{b\bar{b}}}. \quad (5)$$

There are other physics reasons why it is desirable to tag the recoil protons in double diffractive processes. First, it offers a valuable experimental probe of the opacities $\Omega_i(s, b_i^2)$ of the proton. The relevant Feynman diagrams for process (1) are shown in Fig. 1. There is appreciable interference between the amplitudes without and with the soft rescattering corrections, which are shown in Figs. 1a and 1b respectively. We will show that the interference depends on the transverse momenta $\vec{p}_{1t}, \vec{p}_{2t}$ of the recoil protons and on the azimuthal angle ϕ between these momenta. This dependence can be used to probe³ the different soft rescattering models and the behaviour of the opacities $\Omega_i(s, b_i^2)$.

Secondly, we need to understand, and if possible to predict, the \vec{p}_{it} behaviour of the diffractive cross sections in order to plan experiments and to evaluate the acceptance and efficiency of the leading proton detectors at the LHC.

The content of the paper is as follows. In Sect. 2 we recall how the bare perturbative amplitude $A^{(a)}$ of Fig. 1a may be calculated, and then in Sect. 3 we illustrate the effect of rescattering corrections in terms of a simple model. Throughout the paper, it is safe to neglect the rescattering of the centrally produced system M on either proton. This system (for example, a Higgs boson, high E_T dijet, etc.) is

³ Another possibility, to probe the opacity of the proton, is to study the process with rapidity gaps mediated by photon exchange [3]. By varying the momentum transfer of the photon we sample different impact parameters b_i and hence scan the opacity $\Omega(s, b_i^2)$

massive and has small size, so, due to colour transparency [14], the cross section $\sigma(Mp)$ is very small. Rescattering is computed realistically in Sect. 4 and the predictions for a general double-diffractive process, $pp \rightarrow p + M + p$, are presented in Sect. 5. A detour is made in Sect. 6 to discuss double-diffractive light meson production, for which data already exist. Of course, this is beyond the region of validity of a perturbative QCD approach, but, surprisingly, the perturbative predictions agree qualitatively with interesting features of these data. Our conclusions are presented in Sect. 7.

2 The bare amplitude

The amplitude $A^{(a)}$ of Fig. 1a, describing the high energy double-diffractive production of a heavy system M , can be expressed in terms of the generalised (skewed) unintegrated gluon densities $f_g(x, x', t, Q_t, \mu)$. Here $\mu \simeq M/2$ is the scale of the hard $gg \rightarrow M$ subprocess, and t is the transverse momentum squared transferred through the ‘hard’ QCD Pomeron (that is the two-gluon system). Essentially the gluon distribution f_g opens up and describes the internal structure of the ‘hard’ QCD Pomeron, whose exchange mediates the diffractive process (1).

For the exclusive reaction (1) the bare amplitude of Fig. 1a is, to single log accuracy, given by [15]

$$A^{(a)} = \frac{1}{N_c^2 - 1} \int \frac{d^2 Q_t}{Q_t^4} f_g(x_1, \dots, Q_t, \mu) \times f_g(x_2, \dots, Q_t, \mu) \mathcal{M} \quad (6)$$

where \mathcal{M} is the matrix element of the hard $gg \rightarrow M$ subprocess. For example, the cross section for the $gg \rightarrow gg$ subprocess, relevant to high E_T dijet production [1, 16, 17], is

$$\frac{d\hat{\sigma}}{dt} = |\mathcal{M}|^2 = \frac{9}{4} \frac{\pi \alpha_s^2}{E_T^4}. \quad (7)$$

For small $|x_i - x'_i|$, which is appropriate for high energy double diffraction, and $t = 0$, the skewed unintegrated density f_g can be calculated from knowledge of the conventional integrated gluon [18, 19]. The precise form of the t dependence of f_g is not well known. Recall, however, that $f_g(\dots, Q_t, \mu)$ contains a Sudakov-like factor $T(Q_t, \mu)$ which reflects the chance that a gluon with transverse momentum Q_t remains untouched in the evolution up to the hard scale μ —a necessary condition for the survival of the rapidity gap, see, for example, [15, 16, 20]. It is this T factor which provides the infrared stability of the Q_t integral of (6)⁴. For example, for the production of a system of mass $M \gtrsim 100$ GeV at the LHC, the saddle point of the Q_t^2 integration occurs at $Q_t^2 \gtrsim 3\text{--}4$ GeV². On the other hand, the transferred momenta satisfy $|t_i| \lesssim 0.5$ GeV², which are small in comparison with Q_t^2 . Therefore it is natural to assume the factorization

$$f_g(x, x', t, Q_t, \mu) = \beta(t) f(x, x', t = 0, Q_t, \mu), \quad (8)$$

⁴ Moreover, the effective anomalous dimension of the gluon distribution additionally suppresses the contribution from the low Q_t domain [20]

where the whole t dependence is given by the effective form-factor $\beta(t)$ of the QCD Pomeron-proton vertex. In other words, we separate the dependence of the $pp \rightarrow p + M + p$ cross section on the transverse variables (t_1, t_2 or $\vec{p}_{1t}, \vec{p}_{2t}$) from the dependence on the ‘longitudinal’ variables (the initial pp energy \sqrt{s} , the mass M and rapidity y of the system M). That is the bare amplitude is given by

$$A^{(a)}(\vec{p}_{1t}, \vec{p}_{2t}) = \beta(t_1)\beta(t_2)A_M \quad (9)$$

where $t_i \simeq -p_{it}^2$, and where $A_M \equiv A^{(a)}(p_{1t} = p_{2t} = 0)$ may be calculated from (6).

3 Absorption correction: a first look

To calculate the absorptive or soft rescattering amplitude $A^{(b)}$ of Fig. 1b, it is convenient to use the momentum representation. We may neglect the spin-flip component in the proton-Pomeron vertex⁵. We perform the detailed calculation in Sect. 4, but, first, we estimate the qualitative features of the rescattering effect by assuming, in this Section, that the amplitude for elastic proton-proton scattering, at energy \sqrt{s} and momentum transfer k_t , has the simplified form

$$A_{pp}(s, k_t^2) = A_0(s) \exp(-Bk_t^2/2). \quad (10)$$

From the optical theorem we have $\text{Im}A_0(s) = s\sigma_{pp}^{\text{tot}}(s)$, and for the small contribution of the real part it is sufficient to use $\text{Re}A_0/\text{Im}A_0 \simeq 0.12$ in the energy regime of interest. B is the slope of the elastic pp differential cross section, $d\sigma_{pp}/dt \propto \exp(Bt)$.

Using the above elastic pp amplitude we may write the rescattering contribution, Fig. 1b, to the $pp \rightarrow p + M + p$ amplitude as

$$A^{(b)} = i \int \frac{d^2k_t}{8\pi^2} \beta(t_1)\beta(t_2)A_M \frac{A_0}{s} e^{-Bk_t^2/2} \quad (11)$$

where now $t_1 \simeq -(\vec{k}_t - \vec{p}_{1t})^2$ and $t_2 \simeq -(\vec{k}_t + \vec{p}_{2t})^2$. If we take an exponential form for the QCD Pomeron vertices,

$$\beta(t) = e^{bt/2}, \quad (12)$$

then the integral in (11) can be evaluated, to give

$$A^{(b)}(\vec{p}_{1t}, \vec{p}_{2t}) = \frac{iA_0}{4\pi s(B+2b)} \exp\left(\frac{b^2|\vec{p}_{1t} - \vec{p}_{2t}|^2}{2(B+2b)}\right) \times A^{(a)}(\vec{p}_{1t}, \vec{p}_{2t}). \quad (13)$$

To gain insight it is useful to compute the numerical value of $A^{(b)}$ at the LHC energy using reasonable values

⁵ This component is expected to be small and consistent with zero. If we note the similarity between the photon and Pomeron vertices then the magnitude of the isosinglet spin-flip amplitude is proportional to $|\frac{1}{2}(\mu_p^a + \mu_n^a)| \lesssim 0.06$, where the anomalous magnetic moments μ^a of the neutron and proton cancel each other almost exactly

of the parameters. We take $b = 4 \text{ GeV}^{-2}$, $B = 20 \text{ GeV}^{-2}$, $\sigma_{pp}^{\text{tot}} = 100 \text{ mb}$ and, for the moment, neglect the real part, $\text{Re}A_0$, of the pp elastic amplitude. We obtain

$$A^{(b)} = -0.73 \exp(C|\vec{p}_{1t} - \vec{p}_{2t}|^2) A^{(a)}, \quad (14)$$

where $C = 0.29 \text{ GeV}^{-2}$. Thus in the back-to-back configuration with $\vec{p}_{1t} \sim -\vec{p}_{2t} \sim 0.5 \text{ GeV}$, the absorptive correction $A^{(b)}$ completely cancels the bare amplitude $A^{(a)}$, and we predict a deep diffractive dip. Moreover we see that the position of the dip depends on the azimuthal angle ϕ between the transverse momenta \vec{p}_{1t} and \vec{p}_{2t} of the tagged protons. For $\phi = 180^\circ$ the momentum transfer occurs mainly through the elastic amplitude A_{pp} , with $|t_1|$ and $|t_2|$ minimized simultaneously, and hence the amplitude $A^{(b)}$ becomes larger.

4 Detailed treatment of rescattering corrections

To make a realistic calculation of the rescattering corrections we must improve the description of pp soft interaction. We use the model of [21]. It embodies (i) pion-loop insertions to the Pomeron trajectory, (ii) two-channel eikonal description of proton-proton rescattering and (iii) high mass diffractive dissociation. The parameters of the model were tuned to describe all the main features of the soft pp data throughout the CERN-ISR to the Tevatron energy interval. In terms of the two channel eikonal the incoming proton is described by two diffractive eigenstates $|\phi_i\rangle$, each with its own absorptive cross section.

The eigenstates were taken to have the same profile in impact parameter space, and absorptive cross sections

$$\sigma_i = a_i \sigma_0 \quad \text{with} \quad a_i = 1 \pm \gamma, \quad (15)$$

where $\gamma = 0.4$ and σ_0 is defined in [21]. That is the two channel opacity is

$$\Omega_{jj'}^{ii'} = \delta_{ii'} \delta_{jj'} a_i a_j \Omega. \quad (16)$$

The impact parameter representation of the elastic amplitude is thus

$$\text{Im} \tilde{A}_{pp}(s, b_t) = s \left(1 - \frac{1}{4} \left[e^{-(1+\gamma)^2 \Omega/2} + 2e^{-(1-\gamma^2) \Omega/2} + e^{-(1-\gamma)^2 \Omega/2} \right] \right). \quad (17)$$

When we allow for the extra $(1 \pm \gamma)^2$ factors, which reflect the different Pomeron couplings to the two diffractive eigenstates in the $pp \rightarrow p + M + p$ production amplitude, that is in the right-hand part of Fig. 1b, we obtain the effective amplitude of pp rescattering,

$$\text{Im} \tilde{A}_{pp}(s, b_t) = s \left(1 - \frac{1}{4} \left[(1+\gamma)^2 e^{-(1+\gamma)^2 \Omega/2} + 2(1-\gamma^2) e^{-(1-\gamma^2) \Omega/2} + (1-\gamma)^2 e^{-(1-\gamma)^2 \Omega/2} \right] \right). \quad (18)$$

The optical density $\Omega(s, b_t^2)$ was given in [21] for Tevatron ($\sqrt{s} = 2$ TeV) and LHC ($\sqrt{s} = 14$ TeV) energies.

As before, we work in momentum space, and replace (10) by

$$A_{pp}(s, k_t^2) = \frac{1}{2\pi} \int d^2 b_t 4\pi \tilde{A}_{pp}(s, b_t) e^{i\vec{k}_t \cdot \vec{b}_t}. \quad (19)$$

In this way we obtain a more realistic evaluation of the rescattering amplitude $A^{(b)}$ of Fig. 1b. However, from the naïve evaluation of Sect. 3, we anticipate that there will still be a strong cancellation between the bare amplitude $A^{(a)}$ and the absorptive correction $A^{(b)}$, originating from the imaginary part of the elastic rescattering A_{pp} .

First, we must introduce the real part of $A_{pp}(s, k_t^2)$. However, it is not justified to use a constant ratio $\text{Re} A_{pp}/\text{Im} A_{pp} \simeq 0.12$ for k_t away from zero. To account for the k_t dependence we use the dispersion relation result, recalling that the total pp cross section increases logarithmically with energy. Then the even-signature amplitude satisfies

$$\text{Re} \tilde{A}_{pp}(s, b_t) = \frac{\pi}{2} s \frac{\partial \left(\text{Im} \tilde{A}_{pp}(s, b_t)/s \right)}{\partial \ln s}. \quad (20)$$

To convert this relation from the impact parameter space amplitude $\tilde{A}_{pp}(s, b_t)$ to the momentum space amplitude $A_{pp}(s, k_t^2)$ we use (19).

Second, we should specify the form of the QCD Pomeron-proton vertex, $\beta(t)$. The most consistent choice is to take the dipole form used in [21]

$$\beta(t) = \frac{1}{(1-t/a_1)} \frac{1}{(1-t/a_2)}. \quad (21)$$

For comparison we also evaluated the $pp \rightarrow p + M + p$ cross section using the alternative form

$$\beta(t) = e^{bt/2} \quad (22)$$

with $b = 4 \text{ GeV}^{-2}$, which is consistent with the $\gamma p \rightarrow J/\psi + p$ HERA data⁶ [22, 23].

5 Predictions for tagged protons at the LHC

We are now in a position to predict the transverse momentum dependence of the outgoing protons in the double-diffractive production of a heavy system of mass M , that is in the process $pp \rightarrow p + M + p$. We show the results in the form

$$M^2 \frac{\partial^4 \mathcal{L}}{\partial y \partial M^2 \partial^2 p_{1t} \partial^2 p_{2t}} = M^2 \frac{\partial^2 \mathcal{L}}{\partial y \partial M^2} F(\vec{p}_{1t}, \vec{p}_{2t}) \quad (23)$$

where $M^2 d^2 \mathcal{L}/dy dM^2$ is the Pomeron-Pomeron luminosity given in [1] and where the factor F contains the explicit \vec{p}_{1t} and \vec{p}_{2t} dependence. The luminosity, given in [1], was

⁶ The latest HERA data for J/ψ elastic photoproduction prefer $b = 4.5 \text{ GeV}^{-2}$. However, for a heavier system, the smaller slope $b = 4 \text{ GeV}^{-2}$ looks more reasonable

integrated over $d^2 p_{1t} d^2 p_{2t}$ with the assumption that the bare amplitude had an exponential t behaviour,

$$A^{(a)} \propto \exp(b_0(t_1 + t_2)/2) \quad (24)$$

with $b_0 = 4 \text{ GeV}^{-2}$. In addition, the soft survival probability $\langle S^2 \rangle$ was averaged over the available t_1, t_2 domain. Here we unfold the luminosity to expose the \vec{p}_{1t} and \vec{p}_{2t} dependence. In order to be able to use the published $M^2 \partial^2 \mathcal{L}/\partial y \partial M^2$ luminosity, we therefore compute

$$F(\vec{p}_{1t}, \vec{p}_{2t}) = \frac{\beta^2(t_1)\beta^2(t_2)}{\langle S^2 \rangle \pi^2/b_0^2} \frac{\partial^2 S^2(\vec{p}_{1t}, \vec{p}_{2t})}{\partial^2 p_{1t} \partial^2 p_{2t}}. \quad (25)$$

From the product of F , computed in this way, and the luminosity given in [1], we obtain the luminosity as a function of \vec{p}_{1t} and \vec{p}_{2t} , as well as of y and M . This resultant luminosity, (23), needs only be multiplied by the appropriate hard subprocess $gg^{PP} \rightarrow M$ cross section⁷ to obtain the differential cross section for any $pp \rightarrow p + M + p$ diffractive process. Various hard subprocess cross sections were listed, and discussed, in [1].

The factor F is plotted in Figs. 2a–c as a function of p_{1t} for three values of $p_{2t} = 0.2, 0.4$ and 0.7 GeV respectively. In each case the factor is shown for $\phi = 0^\circ, 90^\circ$ and 180° , where ϕ is the azimuthal angle between \vec{p}_{1t} and \vec{p}_{2t} . The continuous and dashed curves are obtained using (21) and (22), respectively, for the QCD Pomeron-proton vertex. Recall that the model of [21] was fitted to ‘soft’ diffractive pp data in the region $|t| \leq 0.5 \text{ GeV}^2$, and so, strictly speaking, $\beta(t)$ of (21) should only be applied for $p_t \lesssim 0.7 \text{ GeV}$. However, we hope we can reliably evaluate rescattering corrections up to $p_t \simeq 1 \text{ GeV}$, as the typical values of k_t (the momentum transferred through the elastic amplitude A_{pp} in Fig. 1b), which are controlled mainly by the elastic slope $B/2$, are much less than 1 GeV . As discussed before, the absorptive corrections are stronger in the back-to-back configuration; already for $p_t < 0.7 \text{ GeV}$ the $\phi = 180^\circ$ curves reveal a rich dip structure.

In the final plot, Fig. 2d, we compare the prediction for F obtained using the elastic amplitude determined in the two-channel eikonal model of [21], with a naïve estimate based on a simple one-channel approach where the elastic pp amplitude is given by the Gaussian formula of (10), that is the amplitude is described by single Pomeron exchange. However, we keep the parameters found in [21], that is $\sigma_{pp}^{\text{tot}} = 102 \text{ mb}$, $B = 20.7 \text{ GeV}^{-2}$ and $\text{Re} A_{pp}/\text{Im} A_{pp} = 0.12$ at $k_t = 0$. In both cases we use (22) for $\beta(t)$. The large difference between the realistic and naïve predictions demonstrates their sensitivity to the model used for soft rescattering.

In Fig. 3 we show the azimuthal dependence of the ‘soft’ survival factor

$$S^2(\vec{p}_{1t}, \vec{p}_{2t}) = \frac{|A^{(a)} + A^{(b)}|^2}{|A^{(a)}|^2}, \quad (26)$$

⁷ The notation gg^{PP} is to indicate that the hard gluons, which interact to form the system M , originate within overall (colourless) hard Pomeron exchanges

p_{1t}, p_{2t} - dependence of the diffractive cross section

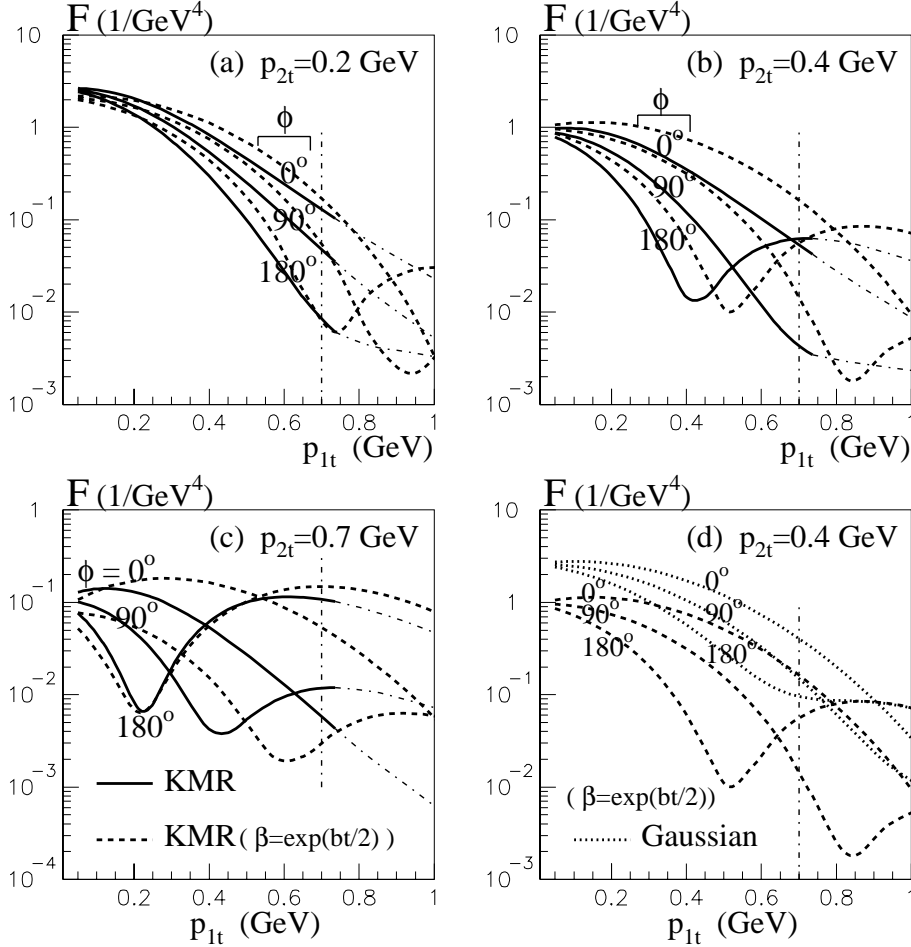


Fig. 2a–d. The factor $F(\vec{p}_{1t}, \vec{p}_{2t})$ of (23) and (25), which specifies the forward going proton transverse momentum dependence of the $pp \rightarrow p + M + p$ cross section, for typical values of p_{1t}, p_{2t} and the azimuthal angle ϕ . The first three plots correspond to $p_{2t} = 0.2, 0.4, 0.7$ GeV respectively, and show the results obtained using the KMR two-channel eikonal model of [21] to calculate the soft rescattering, as described in Sect. 4. The dashed curves show the sensitivity to the form of the QCD Pomeron-proton vertex $\beta(t)$, by replacing the dipole form (21) by the exponential form (22). The dotted curves in **d** correspond to the use of a naïve single-channel eikonal model (with $A^{(b)}$ computed from (10) and (11)) as compared to that obtained with the ‘realistic’ two-channel eikonal model of [21]; in both cases the exponential form factor was used, so the dashed curves are the same in plots **d** and **b**

as a function of the azimuthal angle ϕ , for different choices of p_{1t} and p_{2t} . The rich structure of S^2 is apparent, which feeds through into the double-diffractive cross section. As anticipated, we observe a flatter behaviour in ϕ for small p_{1t} and p_{2t} , while for larger $p_t \sim 0.7$ GeV a diffractive dip already occurs for $\phi \sim 90^\circ$.

6 Application to double diffractive meson production

An interesting ϕ behaviour has been observed by the WA102 collaboration at CERN [24] at lower energies ($\sqrt{s} \sim 30$ GeV) in fixed target central double-diffractive meson production,

$$pp \rightarrow p + X + p, \quad (27)$$

where a partial wave analysis of the X channel allows the identification of a wide range of meson resonances.

It has been emphasized in [25] that within the Regge framework the Reggeon-Reggeon \rightarrow meson vertex, $V(RR \rightarrow X)$, embodied in the amplitude $A^{(a)}$, may contain an azimuthal dependence like

$$|V|^2 = 1 + a \cos \phi + b \cos^2 \phi. \quad (28)$$

In fact, with an appropriate choice of parameters, a phenomenological description of the ϕ dependences observed in the meson-production data can be achieved without any rescattering corrections [25].

For a hard subprocess at scale $\mu = M/2$ with $Q_t^2 \gg |t_i|$ we have no such dependence in the vertex $V(\mathbb{P}\mathbb{P} \rightarrow M)$; the coefficients in (28) satisfy $a, b \lesssim |t_i|/4Q_t^2$. On the other hand, at least part of the azimuthal effects observed in the meson data [24] may originate in the rescattering corrections discussed in the present paper.

To study this further, we adopt the perturbative QCD viewpoint, which offers a dynamical basis in which to understand the structure of process (27). Of course, it is questionable to use perturbative QCD to describe the production of rather light mesons, via (27), where we have no hard scale. On the other hand it is natural to expect a smooth matching between the ‘soft’ and perturbative regimes. In this way we may obtain a qualitative interpretation of observed features the data. As we shall see below, this indeed turns out to be the case.

Recall that, in general, for forward going protons ($p_{it} \ll Q_t$), two ‘hard’ QCD Pomerons can produce only a P-even state with the longitudinal projection of its spin $J_z = 0$ [9, 26]. Also note that, as the QCD Pomerons

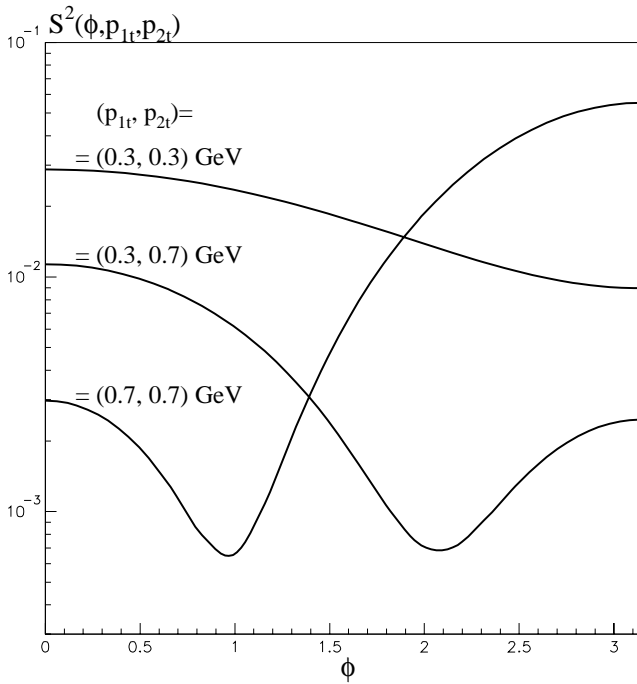


Fig. 3a–d. The dependence of the survival probability, S^2 , of the rapidity gaps on the azimuthal angle ϕ between the transverse momenta \vec{p}_{it} of the forward going protons in the process $pp \rightarrow p + M + p$, for typical values of p_{1t} and p_{2t}

are built from gluons, the underlying fusion subprocess $gg^{PP} \rightarrow X$ may provide a favourable environment for the production of exotic meson states containing gluons (such as glueballs, hybrids, etc.); the cross section of the $gg^{PP} \rightarrow q\bar{q}$ subprocess is much smaller than that of $gg^{PP} \rightarrow gg$, especially in the $J_z = 0$ channel. Next for $J_z = 0$ the vertex $gg^{PP} \rightarrow X(2^{++})$ is strongly suppressed if the 2^{++} state is a normal non-relativistic $q\bar{q}$ meson⁸. This is the result of gauge invariance. Indeed, for X made from a non-relativistic $q\bar{q}$ pair, the fusion process $gg^{PP} \rightarrow (q\bar{q})$ looks like a single local vertex. The distance between the two gluon vertices is of the order of the inverse constituent quark mass ($1/m_q$), which is much smaller than the size of the $(q\bar{q})$ bound state. Now, the structure of the local $gg^{PP} \rightarrow X(2^{++})$ interaction is fixed by gluon gauge invariance. Then the requirement that the polarization tensor $T_{\mu\nu}$ of the 2^{++} meson satisfies $T_{\mu\mu} = 0$ means that the vertex vanishes for $J_z = 0$ [29]. The consequence is that the forward double-diffractive production of normal quarkonium $q\bar{q}(2^{++})$ states should be suppressed [9, 29], and so Pomeron-Pomeron fusion produces relatively more exotic (non- $q\bar{q}$) mesons, such as glueballs, $(q\bar{q}g)$ states, etc. In other words the process $pp \rightarrow p + X(2^{++}) + p$ indeed acts as a filter for separating out exotic mesons from normal mesons [30].

The next observation is that mesons produced in the process $pp \rightarrow p + X + p$ by Pomeron-Pomeron fusion have

⁸ The origin of this result can actually be traced to the absence of the $\gamma\gamma$ decay mode of 2^{++} positronium in the $J_z = 0$ state [27], and then to the absence of the gg decay of a $J_z = 0$ $q\bar{q}$ system [28]

larger transverse momenta, P_t , where $P_t = |\vec{p}_{1t} + \vec{p}_{2t}|$. The reasons are that (i) the $J_z = 0$ selection rule is absent at larger p_{it} , (ii) for a 1^{++} meson, the vertex contains a factor $\epsilon^{\mu\nu\alpha\beta} p_{1t\mu} p_{2t\nu}$ and so prefers larger p_{it} ⁹, and, finally, (iii) heavier (exotic) mesons¹⁰ tend to have larger P_t due simply to kinematics.

Inspection of Fig. 3 shows that for small p_{it} the cross section decreases with increasing ϕ , while for large p_{it} it increases. In the latter domain the dominant contribution comes from the back-to-back configuration.

All the qualitative features described above are indeed observed in the available data [24] for process (27):

- (i) Pomeron-Pomeron fusion in double-diffractive meson production may act as a glueball filter: the final state is enriched by non- $q\bar{q}$ mesons, which have smaller P_T and are produced mainly with tagged protons in the $\phi = 0$ configuration;
- (ii) the normal $q\bar{q}$ light mesons have larger P_T and their cross sections peak at $\phi = 180^\circ$ ¹¹;
- (iii) the 2^{++} channel is produced mainly in the $J_z = 0$ state [32].

These expectations can be confirmed by observing the double-diffractive production of heavier quarkonia, like χ_c and χ_b , at the Tevatron and at RHIC. The heavier mesons sample smaller distances and so their production should be better described by perturbative QCD. Of course, χ_c is probably still not heavy enough, but nevertheless it would be interesting to compare $\chi_c(2^{++})$ production with the enhanced 2^{++} glueball production rate.

7 Conclusions

It is well known that, in general, absorptive effects in inelastic diffractive processes are much stronger than in the elastic amplitude (see, for example, [33]). Such rescattering clearly violates Regge factorization and leads to non-trivial correlations between the transverse momenta \vec{p}_{1t} and \vec{p}_{2t} of the forward going protons in processes of the type $pp \rightarrow p + M + p$. Measuring the p_{it} and the azimuthal angle ϕ distributions can provide an interesting possibility to probe the opacity $\Omega(s, b_t)$ of the incoming proton and, moreover, to test the dynamics of soft rescattering.

One of the best examples to study these effects is exclusive high- E_T dijet production, $pp \rightarrow p + \text{dijet} + p$, where the cross section for the hard subprocess is large and well known.

Although questionable, the above perturbative formalism was applied to central double-diffractive meson pro-

⁹ By analogous arguments, the forward production of the unnatural spin-parity states, 0^{-+} and 2^{-+} , should be strongly suppressed and also favours large p_{it} . This does not depend on whether or not the mesons are quarkonium states. Also, 1^{-+} production would tend to occur at large p_{it}

¹⁰ This, of course, is also valid for 0^{++} mesons

¹¹ The preference for double-diffractive $f_2(1270)$ -meson production in the $\phi > 90^\circ$ domain has been observed at higher energies at the ISR [31]

duction at lower energies, at which data exist. Surprisingly, the qualitative features of these data were reproduced.

Acknowledgements. We thank Frank Close, Jerry Lamsa, Risto Orava and Albert de Roeck for interesting discussions. One of us (VAK) thanks the Leverhulme Trust for a Fellowship. This work was partially supported by the UK Particle Physics and Astronomy Research Council, by the Russian Fund for Fundamental Research (grants 01-02-17095 and 00-15-96610) and by the EU Framework TMR programme, contract FMRX-CT98-0194 (DG 12-MIHT).

References

1. V.A. Khoze, A.D. Martin, M.G. Ryskin, Eur. Phys. J. C **23**, 311 (2002)
2. K. Piotrkowski, Phys. Rev. D **63**, 071502 (2001); hep-ex/0201027
3. V.A. Khoze, A.D. Martin, M.G. Ryskin, hep-ph/0201301, Eur. Phys. J. C, in press
4. Yu.L. Dokshitzer, V.A. Khoze, T. Sjöstrand, Phys. Lett. B **274**, 116 (1992)
5. J.D. Bjorken, Int. J. Mod. Phys. A **7**, 4189 (1992); Phys. Rev. D **47**, 101 (1993)
6. H. Chehime, D. Zeppenfeld, Phys. Rev. D **47**, 3898 (1993)
7. R.S. Fletcher, T. Stelzer, Phys. Rev. D **48**, 5162 (1993)
8. E.M. Levin, hep-ph/9912402 and references therein
9. V.A. Khoze, A.D. Martin, M.G. Ryskin, Eur. Phys. J. C **19**, 477 (2001); erratum, ibid. C **20**, 599 (2001)
10. M.M. Block, F. Halzen, Phys. Rev. D **63**, 114004 (2001)
11. E. Gotsman, E. Levin, U. Maor, Phys. Rev. D **60**, 094011 (1999) and references therein
12. A.B. Kaidalov, V.A. Khoze, A.D. Martin, M.G. Ryskin, Eur. Phys. J. C **21**, 521 (2001) and references therein
13. V.A. Khoze, hep-ph/0105224
14. A.B. Zamolodchikov, B.Z. Kopeliovich, L.I. Lapidus, JETP Lett. **33**, 595 (1981); G. Bertsch, S.J. Brodsky, A.S. Goldhaber, J.F. Gunion, Phys. Rev. Lett. **47**, 297 (1981)
15. V.A. Khoze, A.D. Martin, M.G. Ryskin, Eur. Phys. J. C **14**, 525 (2000)
16. V.A. Khoze, A.D. Martin, M.G. Ryskin, Phys. Rev. D **56**, 5867 (1997)
17. A. Berera, J.C. Collins, Nucl. Phys. B **474**, 183 (1996)
18. A.D. Martin, M.G. Ryskin, Phys. Rev. D **64**, 094017 (2001)
19. A.G. Shuvaev, K.J. Golec-Biernat, A.D. Martin, M.G. Ryskin, Phys. Rev. D **60**, 014015 (1999)
20. V.A. Khoze, A.D. Martin, M.G. Ryskin, Phys. Lett. B **401**, 330 (1997)
21. V.A. Khoze, A.D. Martin, M.G. Ryskin, Eur. Phys. J. C **18**, 167 (2000)
22. H1 Collaboration: S. Aid et al., Nucl. Phys. B **472**, 3 (1996); H1 Collaboration: C. Adloff et al., Eur. Phys. J. C **10**, 373 (1999); Phys. Lett. B **483**, 23 (2000); ZEUS Collaboration: J. Breitweg et al., Z. Phys. C **75**, 215 (1997); Eur. Phys. J. C **6**, 603 (1999)
23. A. Levy, Phys. Lett. B **424**, 191 (1998)
24. WA102 Collaboration: D. Barberis et al., Phys. Lett. B **467**, 165 (1999); ibid. B **474**, 423 (2000); ibid. B **484**, 198 (2000); ibid. B **488**, 225 (2000)
25. F.E. Close, A. Kirk, G. Schuler, Phys. Lett. B **477**, 13 (2000); F.E. Close, Acta Phys. Polon. B **31**, 2557 (2000); F.E. Close, A. Kirk, Phys. Lett. B **485**, 24 (2000)
26. V.A. Khoze, A.D. Martin, M.G. Ryskin hep-ph/0006005, in Proc. of 8th Int. Workshop on Deep Inelastic Scattering and QCD (DIS2000), Liverpool, eds. J. Gracey, T. Greenshaw (World Scientific, 2001), p.592
27. K.A. Tumanov, Zh. Eksp. Teor. Fiz. (USSR), **25**, 385 (1953); A.I. Alekseev, Sov. Phys. JETP **7**, 826 (1958)
28. M. Krammer, H. Krasemann, Phys. Lett. B **73**, 58 (1978)
29. Feng Yuan, Phys. Lett. B **510**, 155 (2001)
30. F.E. Close, A. Kirk, Phys. Lett. B **397**, 333 (1997)
31. A. Breakstone et al., Z. Phys. C **48**, 569 (1990)
32. WA102 Collaboration: D. Barberis et al., Phys. Lett. B **453**, 305 (1999); 316
33. A.B. Kaidalov, Phys. Rep. **50**, 157 (1979); Ya.I. Azimov, V.A. Khoze, E.M. Levin, M.G. Ryskin, Nucl. Phys. B **89**, 508 (1975)